Design: An algorithm for testing of HER-2/neu at our institution was establshed. Newly diagnosed invasive breast cancers initially undergo HER-2/neu protein testing by immunohistochemistry (IHC, HercepTest, DakoCytomation). Tumors with equivocal IHC results (weak 2+ signal, heterogeneous signal, indeterminate signal such as edge effect) will undergo second testing by FISH (PathVysion, Vysis). Tumor's parameters were recorded including tumor's Nottingham grade, IHC score and FISH score.
Results: A group of 30 breast cancers was used as a validation set prior to implemeting FISH testing. 100% correlation rate was achieved between our lab and the reference lab prior to implementing FISH procedure locally. After the first 200 tests were conducted, FISH testing failure rate averages at < 1%, substantially lower than the national average failure rate of 10%.
Conclusions: Local testing of HER-2/neu by FISH is not only possible but can be more successful than in central laboratories. Part of the success is due to (a) the more homogeneous tissue fixation and processing procedures in the local setting compared to the central setting where specimens are received from a very large pool of histology laboratories, and (b) the necessary FISH testing and interpretation experience of our pathologists prior to implementing the test locally. We believe it is crucial to any pathology laboratory who wishes to impelment HER-2/neu testing by FISH to undergo an extensive validation process including at least 20 cases of borderline FISH results, before they proceed with clinical implementation of the test at their institutions.

Cardiovascular

198 Effect of Age on Aortic Intima Thickness and Intimal Soluble Elastin Fragments (sELAF) in Children and Young Adults in a Japanese Population

T Akima, K Nakanishi, H Kishimoto, S Tominaga, S Hiroi, A Suzuki, RJ Siegel, F Ohsuzu, T Kawai, K Suzuki, M Katayama. National Defense Medical College, Tokorozawa, Saitama, Japan; Saitama Children's Medical Center, Saitama, Japan; Cedars-Sinal Medical Center, Los Angeles, CA; Diagnostic Research Laboratory, Eisai, C., Ltd.
Background: Intimal thickening in arterial wall begins in childhood. We have established a monoclonal antibody (HASG61-1) against sELAF using hybridoma technology. This antibody detects sELAF including tropoelastin, but not mature elastin. The purpose of this study was to investigate the relationship between intimal thickening (IT) and aging, and between IT and intimal sELAF in Japanese children and young adults.
Design: We performed quantitative pathologic analysis in human thoracic-abdominal aortic specimens of 104 autopsies (63 boys, age range, 0-18 years) using a computed digitized measuring system, and sELAF using immunohistochemistry.
Results: No atherosclerotic lesion formation was found in any of the specimens. Entire arterial wall thickness (EAWT) correlated with age, height, body weight (BW), and body mass index (BMI) [EAWT (μm) = 606.3+ 16.2× age (year), $R^2 = 0.262$, $p<0.0001$; 417.7+ 2.7 × height (cm), $R^2= 0.254$, $p<0.0001$; 581.8+ 6.5× BW (kg), $R^2 = 0.245$, $p<0.0001$; 533.5+ 12.1× BMI (kg/m^2), $R^2 = 0.051$, respectively]. Furthermore, arterial thickness of intima and media correlated with age [intimal thickness (μm) = 71.2+ 3.2× Age (year), $R^2 =0.99$, $p=0.0011$; medial thickness (μm) = 534.3+ 12.9× Age (year), $R^2 =0.237$, $p<0.0001$, respectively]. Meanwhile, intima/media ratio which is one of markers of atherosclerosis did not change through aging in the normal aorta. By immunohistochemistry, the sELAF were detected densely in the intima and weakly in the media of aorta. However, intimal sELAF did not change with aging.
Conclusions: Intimal thickening of aorta and sELAF detected in the intima occurs in early childhood and progresses with aging. These aortic wall changes are not associated with atherosclerosis but the arterial growth itself.

199 Expression of Soluble Elastin Fragments in Normal Human Aorta and Atherosclerotic Lesions

T Akima, K Nakanishi, K Suzuki, M Katayama, S Hiroi, S Tominaga, T Nishioka, M Kusuhara, RJ Siegel, F Ohsuzu, T Kawai. Cedars-Sinai Medical Center, Los Angeles, CA; National Defense Medical College, Tokorozawa, Saitama, Japan; Eisai Co, Ltd, Tsukuba, Ibaraki, Japan; Saitama Medical Center of Saitama Medical College, Kawagoe, Saitama, Japan.
Background: Elastin is a major extracellular matrix component of arterial wall.
Design: Our aim is to assess the characteristics and roles of immuno-detectable elastin in normal aorta and fibrous, atheromatous and ruptured plaques (FP, AP and RP, respectively), using monoclonal antibodies against solubilized elastin fragments. We examined 172 human aortic specimens from 9 autopsies.
Results: Western blot analysis of the extracts of normal aorta and these plaques revealed several bands from 20 to 65 kDa: the 65 kDa band was tropoelastin. Decreased components in RP were elastin fragments ranging from 35 to 45 kDa. By immunohistochemistry, immuno-detectable elastin was abundantly distributed in the intima of normal aorta, but decreased in the core of AP and RP. The concentrations in RP were significantly lower than those in normal aorta, FP and AP. Elastin mRNA/GAPDH mRNA in FP and AP was significantly higher than that in normal aorta, respectively. Stepwise multivariable analysis showed that the concentrations of immuno-detectable elastin were significantly lower in the plaques having the rupture or large lipid pool than in those without these features.
Conclusions: These results indicate that, in the core area of AP and RP, loss of elastin fragments and negative elastogenesis may predispose in the plaque rupture.

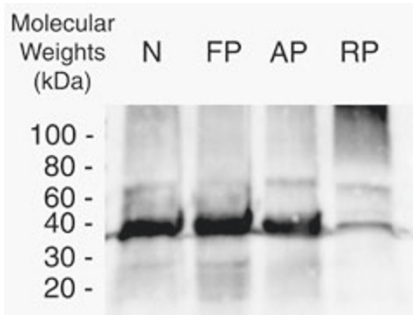

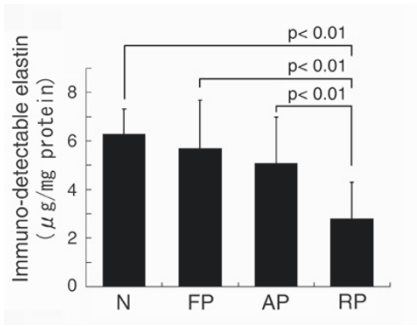

200 Endomyocardial Biopsy To Validate Three-Dimensional Electroanatomic Voltage Mapping as a New Diagnostic Tool To Differentiate Right Ventricular Outflow Tract Tachycardia from Arrhythmogenic Right Ventricular Cardiomyopathy

C Basso, D Corrado, B Tokajuk, L Leoni, A Pavei, G Buja, S Iliceto, G Thiene. University of Padua Medical School, Padova, Italy.
Background: Differential diagnosis between idiopathic right ventricular outflow tract (RVOT) tachycardia (VT) and segmental form of arrhythmogenic right ventricular cardiomyopathy (ARVC) is challenging in the clinical setting.
Design: By a new invasive electrophysiologic technique, ie three-D electroanatomic voltage mapping, the 3-D geometry of the RV depicting the peak-to-peak amplitude of the bipolar electrograms recorded at multiple endocardial sites is constructed. The technique allows to detect low-voltage areas that correspond to regions of myocardial atrophy, ie fibro-fatty replacement in ARVC patients. We assessed whether three-D electroanatomic voltage mapping can differentiate between idiopathic RVOT VT and ARVC by comparing the results with endomyocardial biopsy (EMB). .
Results: 24 consecutive patients (13 M and 11 F, mean age 34±11 years) with recurrent VT from the RVOT, and without echocardiographic evidence of RV dilatation/dysfunction were investigated. Activation mapping showed that all VTs arose from the RVOT. Voltage mapping was normal (>1.5 mV throughout the RV) in 17 of 24 patients (70%, Group A) and abnormal in the remaining 7 patients (30%, Group B), showing 2±1.4 areas with bipolar electrogram amplitude <0.5 mV (electroanatomic scar). Two patients from Group B had abnormalities limited to the RVOT, whereas in the other 5 the disease also involved the anterior (4), the inferobasal (3), and the apical (2) regions. At EMB, 6/7 patients from Group B (86%) versus 0/17 patients from Group A ($p= 0.001$) presented a diagnostic amount of myocardial atrophy (<45% of EMB section area) plus fibro-fatty tissue replacement, thus showing a strong correlation with RV electroanatomic scars. Catheter ablation successfully eliminated VT in 13 of 15 patients. During a follow-up of 26±9 months, 3 out of 7 patients (43%) from Group B received an ICD due to syncope or cardiac arrest, whereas all patients from Group A had an uneventful outcome ($p=0.02$).
Conclusions: Abnormal voltage map were identified in nearly 30% of patients with RVOT VT and no RV dilatation/dysfunction. Electroanatomic scar(s) correlated with myocardial atrophy and fibrofatty replacement at EMB as to confirm an underlying segmental form of ARVC at risk of life-threatening events

201 A Postmortem Investigation of Distal Coronary Microembolization in Acute Coronary Syndromes

C Basso, F Bacchion, A Ramondo, L Cacciavillani, G Tarantini, A Abudureheman, R Razzolini, S Iliceto, G Thiene. University of Padua Medical School, Padova, Italy.
Background: Embolization of athero-thrombotic debris occurs in the setting of acute coronary artery thrombosis. Aim of our study was to evaluate the distal intramyocardial vessels in acute coronary syndromes in order to assess prevalence and features of coronary microembolization
Design: 60 pts who died due to an acute coronary syndrome (acute myocardial infarction-AMI- or sudden coronary death-SCD) with documented coronary artery thrombosis were evaluated; they consisted of 10 AMI pts who had thrombolysis (*Group A*, 5M-5F, mean age 68,5±14), 20 pts who underwent primary percutaneous coronary intervention (PCI) (*Group B*, 15M-5F, mean age 67±10), 18 AMI pts without coronary revascularization (*Group C*, 14M-4F, mean age 72±10) and 12 SCD pts (Group D, all M, mean age 33±10). Blocks of myocardium taken from both the perfusion territories of

the culprit coronary segments and unrelated ones were evaluated. All samples were sectioned at 5 micron intervals and stained with H&E, trichrome, and a panel of ICH antibodies (vWF, CD31, CD61, fibrin).
Results: Luminal thrombosis in the culprit coronary segments was occlusive in 35% and mural in 65%. Platelet/fibrin microemboli were detected within the perfusion territories of a thrombosed coronary segment in 40% of the cases. However, their spatial distribution in the related myocardium was not widespread but mild focal. Microembolization occurred in 50% of Group A, 55% of group B, 22% of group C and 33% of group D. Overall, its prevalence was higher in the revascularized vs the untreated pts (53% vs 26%, p=0.03) but no difference was found between revascularized pts with thrombolysis (50%) and those with PCI (55%, p=0.4). Distal coronary microembolization was detected in 51% of cases with residual mural thrombosis vs 19% of cases with occlusive thrombosis (p=0.03).
Conclusions: Distal coronary microembolization is a common finding in acute coronary syndromes and, although it occurs also spontaneously as a result of physiologic wash-out of atherothrombotic material, its frequency is higher after recanalization procedures either pharmacologic or interventional. However, its focal distribution in the related myocardium suggests that distal coronary microembolization probably plays a minor role and additional factors are involved in microcirculatory impairment after recanalization procedures.

202 Primary Bioptic Malignant Cardiac and Pericardial Tumors. A 35 Years Single Institution Survey

C Basso, M Valente, G Gerosa, G Thiene. University of Padua Medical School, Padova, Italy.
Background: Primary cardiac and pericardial tumors (CPT) are rare and even less common are malignant ones. Aim of our study was to assess the prevalence and histotype of malignant forms among a consecutive series of primary CPT examined in a single Institution.
Design: In the time interval 1970-2004 among 188 consecutive pts who had an in vivo diagnosis of primary CPT, either by surgical pathology and/or endomyocardial biopsy investigation, 19 (10%) had a malignant form. They were 9 females and 10 males, age ranging from 21 to 80 yrs (mean 52±12). Besides gross and histologic examination, tumour histotype was defined by immunohistochemistry using a large panel of antibodies and by transmission electron microscopy.
Results: Primary malignant CPT comprised 6 extracardiac (3 pericardial mesothelioma and 3 pulmonary artery sarcoma) and 13 intracardiac masses. The latter group consisted of angiosarcoma of the right atrium +/-right ventricle (3), undifferentiated myxoid sarcoma of the left atrium (3), malignant fibrous histiocytoma of the left or right atrium (2), leiomyosarcoma of the right ventricle or left atrium (2), fibrosarcoma of the right atrium (1), B cell lymphoma of the right atrium (1) and left atrial schwannoma (1). In four patients (40%) a preoperative histologic diagnosis was achieved by transvenous endomyocardial biopsy (all right-sided tumors). Noteworthy, five malignant primary CPT, all located in the left atrium, had a preoperative misdiagnosis of cardiac myxoma. Surgical resection was performed in all but two pts. All pts died with a maximum survival time of 24 months, except a 21 year old woman with left atrial leiomyosarcoma who is alive without any evidence of tumor recurrence at 24 mos follow-up after surgical resection and adjuvant anthracycline based chemotherapy.
Conclusions: Primary malignant CPT represent 10% of all primary CPT in our series. The prognosis is poor and generally measured in months, independently from the tumour histotype and from surgical resection and chemotherapy. Endomyocardial biopsy is a safe procedure to achieve an in vivo diagnosis in the setting of right intracavitary masses. Intracavitary atrial malignant tumors may mimic cardiac myxoma and differential diagnosis is achievable only by a thorough microscopic and immunohistochemistry study of surgical resections.

203 Cardiomyocyte Basement Membrane Integrity Is Affected after Left Ventricular Unloading in End Stage Heart Failure: The Role of MMP-2

AH Bruggink, MFM van Oosterhout, N de Jonge, JPM Cleutjens, DF van Wichen, J van Kuik, FHJ Gmelig-Meyling, R de Weger. University Medical Center, Utrecht, Netherlands; UMCU, Utrecht, Netherlands; UM, Maastricht, Netherlands.
Background: Left ventricular assist devices (LVAD) are commonly used in patients with heart failure as a bridge to heart transplantation. After LVAD implantation heart size tends to normalize. During this process of reverse remodeling cardiomyocytes decrease in size and extracellular matrix (ECM) volume increases. The interface between the cardiomyocytes and ECM like the basement membrane (BM) and transmembrane proteins like integrins might undergo structural and functional changes during this process. Therefore, we studied the changes of the BM, of collagen IV, a major BM component and of Matrix Metallo Proteinase-2 (MMP-2) which is involved in collagen breakdown.
Design: LV tissue was obtained from 25 patients with refractory end-stage heart failure at time of LVAD implantation and after 35-557 days at time of heart transplantation. BM was studied using immunohistochemical staining with collagen IV and by Transmission Electron Microscopy (TEM). Collagen IV and MMP-2 was quantified at the transcriptional and protein level by Q-PCR andWestern Blot, and gelatin Zymography, respectively.
Results: Pre-LVAD LV biopsies showed ultrastructurally an irregular and dispersed BM and connection of collagen fibers from the ECM to the BM of cardiomyocytes. Post-LVAD the BM was regular along the cardiomyocyte but collagen fibers connecting to the BM were only rarely observed. The thickness of the BM was decreased (n=5, p=0.02) with a significant reduced immunoreactivity for type IV collagen in the BM after LVAD support. However, there was no difference in type IV collagen mRNA expression pre- and post-LVAD. In failing hearts, pre LVAD MMP-2 mRNA was ~3 times increased compared to normal controls (p<0.01) and increased a further 2 times Post- LVAD (p=0.01). This increase was confirmed at the protein level by Western blot. In addition, only post-LVAD an active MMP-2 band was present in gelatin zymography. The active MMP was localized in the BM of the cardiomyocyte as was shown by type IV collagen In Situ Zymography
Conclusions: The structural changes of the basement membrane during LVAD therapy in heart failure are at least in part the result of an increased MMP-2 activity, and not due to a reduced synthesis of type IV collagen. Supported by the Netherlands Heart Foundation grant 2004T31.

204 Pulmonary Artery Sarcoma: A Follow-Up Study of 22 Cases

AP Burke, JC Fanburg-Smith, JF Fetsch, M Miettinen. University of Maryland Medical System, Baltimore, MD; Armed Forces Institute of Pathology, Washington, DC.
Background: Sarcomas arising from the intima of the pulmonary artery are rare. These typically present as chronic pulmonary embolism. There are few follow-up studies that clearly separate sarcomas arising from the artery from equally rare pulmonary parenchymal sarcomas.
Design: We retrospectively identified sarcomas of the pulmonary artery from our files. Origin from the pulmonary artery was confirmed by histologic and/or radiology data. Survival data was analyzed using Kaplan-Meier statistics.
Results: Twenty-two cases with available follow-up were included. There were eight women (50 +/-16), and 14 men (49 +/- 19). Site of origin was left pulmonary artery (8), right pulmonary artery (4), pulmonary trunk (7), pulmonary trunk extending into right pulmonary artery (1), pulmonary trunk extending into left pulmonary artery (1), and pulmonary trunk, extending into both pulmonary arteries (1). Tumor mean size was 4.7 centimeters. Histologically, the tumors were undifferentiated sarcomas with variable pleomorphism (16), three of which were diffusely myxoid; undifferentiated sarcoma with areas of osteo- or chondrosarcoma (5), and low-grade myofibroblastic tumor, without necrosis (1). All cases studied were positive for vimentin, focally for actin, and negative for desmin, S100 protein, and Factor VIII rag. Except the one low-grade sarcoma, all were considered high-grade. Follow-up data was obtained on all cases (range, 2 weeks - 96 months). Survival was poor (median 11 months), with all but one patient dead of disease. Only one patient, with a low grade sarcoma of myofibroblastic phenotype, is alive and well at 11 years. Range of survival until death from disease was 2 weeks to 96 months. Gender, race, tumor histology (mitotic count, presence of necrosis), size, and tumor site or extension had no effect on survival. Only advancing patient age had an adverse effect on survival (p<.001).
Conclusions: Pulmonary artery sarcoma is generally a high grade undifferentiated spindle cell tumor, sometimes with osteo- or cartilaginous differentiation. These mainly occur in adults, with a male predominance and overall poor prognosis, as most patients die of disease within 3 years. However, exceedingly rare low-grade sarcomas may arise from the pulmonary artery intima, which may have favorable behavior.

205 Incidence of Endothelialitis in Cardiac Allograft Biopsies, and Relationship to C4d Deposition and Clinical Evidence of Humoral Rejection

AP Burke, FR Tavora, J Papadimitriou, CI Drachenberg. University of Maryland Medical Center, Baltimore, MD.
Background: The incidence of endothelialitis in cardiac transplants, and the relationship to clinical symptoms and humor rejection, is unclear.
Design: 141 sequential biopsies from 54 cardiac allograft recipients were prospectively studied. Rejection was graded according to ISHT criteria, and inflammatory infiltrates characterized by immunohistochemical staining for CD3, CD4, CD8, CD68 and CD20. Endothelialitis was defined as lymphocyte infiltrates within capillary, arteriolar or venular walls, with endothelial swelling. Complement C4d was identified in capillary walls by immunofluorescent staining and immunohistochemical staining on paraffin sections.
Results: Endothelialitis was identified in 9 biopsies (6%) of 5 patients (9%). ISHT rejection grades were 0 (2 biopsies) 1A (2 biopsies) and 1B (5 biopsies) Immunofluorescence staining was present in 3 of 5 patients (2+ diffuse in 2, 1+ focal in one). Immunohistochemical staining for C4d was negative in every case. One patient had suspected humoral rejection (with 2+ diffuse C4d staining by immunofluorescence), based on serologic presence of preformed antibodies to class II HLA antigens. This patient was treated with plasmaphoresis; the other patients were doing well clinically without evidence of humoral rejection, and were not treated for humoral rejection. The endothelial infiltrates were CD3, CD4, and CD8 +, with only occasional CD57+ cells.
Conclusions: Endothelialitis is present in a <10% of heart transplant recipients. A high proportion demonstrate C4d capillary deposition by immunofluorescence staining, but only a few show humoral rejection clinically. The eventual risk for developing graft vascular disease remains undetermined.

206 Failure To Detect HSV, CMV and EBV Viral Genomes in Giant Cell Arteritis Biopsies

M Cankovic, RJ Zarbo. Henry Ford Hospital, Detroit, MI.
Background: Giant cell arteritis (GCA) or temporal arteritis (TA) is a chronic vasculitis of large and medium sized arteries. Except for the histopathology of the arterial wall, there are no diagnostic tests that can be widely used for diagnosing GCA. Additionally, a high percentage of patients present with non-specific symptoms that do not conform to any specific set of criteria. Direct evidence for detection of human herpes simplex virus (HSV) in association with GCA was recently reported (Powers JF *et al*. Am J Clin Pathol 2005;123:261-264)), while previous reports failed to detect presence of herpes viruses in GCA (Helweg-Larsen *et al*. J Rheumatology 2002;41:445-449). For this study we sought to determine by molecular techniques whether HSV DNA could be detected in temporal artery biopsies from patients with pathologically confirmed GCA, or if cytomegalovirus (CMV) or Epstein-Barr virus (EBV), both of which have been implicated in etiology of cardiovascular disease, might be involved.
Design: We selected 35 cases of biopsy confirmed GCA from the HFH archives. We also selected 9 control cases: giant cell myocarditis (2), arterial biopsy specimens with no

inflammation (6), skin biopsies with granulomatous inflammation (2), and a bone-soft tissue biopsy with inflammation (1). Sections were cut from formalin fixed, paraffin embedded (FFPE) tissue blocks, and DNeasy mini kit (Qiagen) was used for DNA isolation. Viral detection was done using quantitative real-time PCR (QPCR). Two kinds of probes were used for this assay: 1) Dual labeled TaqMan probes for HSV1, CMV and EBV detection, and an Eclipse MGB probe (Nanogen) for HSV ½ detection. All samples were analyzed on Rotor Gene 3000 (Corbett Research). To establish the sensitivity limits of the assays, we serially diluted positive control standards, which were also isolated from FFPE specimens, and were able to detect as few as 1 viral copy/ul by the same QPCR protocols.

Results: We failed to detect the presence of HSV genome in any of the study or control samples tested. CMV testing was positive in one case of giant cell arteritis. EBV testing only gave positive results for the two skin biopsy specimens, and was negative in all the other specimens.

Conclusions: We found no evidence of DNA from HSV or EBV in any of the inflamed temporal arteries. The sole CMV positive case does not provide sufficient proof for CMV involvement in GCA. Our results indicate that these agents do not seem to play a unique or dominant role in pathogenesis or molecular diagnosis of GCA.

207 Clinicopathologic Findings in 111 Consecutively Excised Ascending Aortic Aneurysms

MJ Collins, V Dev, PWM Fedak, JW Butany. Toronto General Hospital, University of Toronto, Toronto, ON, Canada; Toronto General Hospital, Toronto, ON, Canada.

Background: The pathogenesis of ascending aortic aneurysms (AA) is poorly understood yet large studies documenting the histological features of ascending AA are lacking. We examined histological changes in a large consecutive series of surgically excised ascending AA.

Design: A total of 111 consecutive patients with surgical excision of ascending AA between 2002-2004 were studied. Tissue was received as a continuous ring, processed for routine histology and stained with hematoxylin and eosin and movat pentachrome. A blinded analysis was performed and the tissue samples graded for elastic laminae fragmentation, elastic tissue integrity, smooth muscle cell (SMC) abundance, inflammatory cell infiltration and the presence of intemal changes. Relevant clinical data included native aortic valve morphology, history of hypertension, and Marfan syndrome.

Results: Mean patient age at surgery was 58.7+/-15.6 years and was not significantly different between any of the groups studied. Histological characteristics are summarized in Table 1. Inflammatory cell infiltration was present in 80 (72.1%) of all patients and localized mainly to the adventitia. Some degree of intemal change was observed in 93 (83.8%) of all patients though complex atherosclerosis was rare. Patients with a bicuspid aortic valve (BAV) showed better preservation of the elastic laminae and lower occurrence of intemal changes compared with tricuspid aortic valves (TAV). Female gender and Marfan syndrome were associated with more severe changes in the aortic wall, while advanced patient age was associated with more severe loss of SMC but not elastic tissue compared with younger patients.

Conclusions: The histological appearance of ascending AA is highly variable and reflects underlying patient characteristics. These results suggest that mechanisms of AA development may be highly divergent.

Table 1

	n (% of all patients)	Elastin Loss	Elastin Fragmentation	SMC Loss	Intimal Changes Present
BAV	34 (30.6%)	0.7 *	2.4 *	1.6	64.7% **
TAV	71 (64.0%)	1.8 *	2.7 *	1.8	93.0% **
Female	37 (33.3%)	1.9 *	2.7 *	2.1 *	89.2%
Male	74 (66.7%)	1.2 *	2.5 *	1.7 *	80.1%
Marfan	12 (10.1%)	2.0 *	2.9 *	1.5 *	83.3%
Non-Marfan	99 (89.9%)	1.3 *	2.5 *	1.9 *	82.8%
Age > or equal to 65	46 (41.4%)	1.6	2.5	2.0 *	87.0%
Age < 65	65 (58.6%)	1.3	2.6	1.7 *	81.5%

* = p<0.05 on unpaired t-test, ** = p < 0.05 on Fisher's exact test

208 The Angiotensin Converting Enzyme DD Polymorphism Is Increased in Frequency in Sudden Coronary Death Due to Stable Plaque and Is Associated with Increased Plaque Burden

W Creighton, AP Burke, B Kutys, R Virmani. University of Maryland Medical Center, Baltimore, MD; International Registry of Pathology, Gaithersburg, MD.

Background: Polymorphisms of the ACE gene are associated with increased plasma ACE concentration and increased plaque burden in patients with coronary artery disease. Various polymorphisms of the genes involved in the RAS, especially the DD genotype of ACE, have been proposed as a genetic marker for increased risk of coronary atherosclerosis. ACE expression has been demonstrated in macrophages, T-cells, and endothelial cells in coronary and carotid plaques and may contribute to progression of atherosclerosis. The DD genotype has not been studied in autopsy material from sudden coronary death and compared to controls.

Design: Frozen splenic or renal tissues from sudden unexpected death victims > 30 years were collected prospectively. After full cardiac examination and forensic autopsy, cases were classified as coronary deaths with thrombus (n=110), coronary deaths without thrombus (n=79), and non-coronary deaths (n=212). Coronary plaque burden was estimated in hearts from patients > 40 years of age (sum of maximal % luminal narrowing in each 4 epicardial artery, left main, left anterior descending, left circumflex, and right). Genomic DNA will prepared from human splenic tissues by standard methods. The DD polymorphism (M235T) of the ACE gene was be determined by PCR. The PCR products were purified on Microcon (Millipore, Billerica, MA), and directly sequenced using an ABI 377 automated sequencer.

Results: The DD polymorphism was present in 23%, ID 61%, and II 16% of all cases examined. The proportion of DD in coronary thrombus deaths was 23%, coronary deaths without thrombus 32%, and noncoronary deaths 21% (p>0.1). In whites, DD was present in 34% of coronary deaths without thrombus, 19% of coronary thrombus deaths, and 14% of controls (p=.01, coronary non-thrombus vs. coronary thrombus deaths; p=.05, coronary non-thrombus vs. controls). Plaque burden was greatest in patients with DD genotype (158 ± 17) compared to II (142±23) and ID (114±12). In whites, plaque burden in the DD genotype (201±25) was greater than ID (134±16, p=.03) and II (131±26, p=.06).

Conclusions: The DD polymorphism, in whites, is associated with sudden death due to coronary disease without thrombus, and increased coronary atherosclerotic plaque burden.

209 Native Valvular Pathology and Pannus Overgrowth in Explanted Prosthetic Heart Valves

KS Cunningham, M Borger, S Leong, J Butany. University Health Network, Toronto General Hospital, University of Toronto, Toronto, ON, Canada.

Background: Host tissue overgrowth (pannus) is a virtually ubiquitous response to prosthetic devices implanted within the cardiovascular system. Occasionally the magnitude of pannus overgrowth interferes with mechanical or bioprosthetic heart valve function causing impaired cardiac performance and device failure. The etiology of tissue overgrowth is unclear; however, local endocardial factors and systemic hemodynamics initiated by the antecedent cardiac pathology may contribute.

Design: Explanted mechanical and bioprosthetic heart valves from patients for whom the native valve pathology was available, from 1990-2005, were examined grossly and microscopically to assess the degree of tissue overgrowth (mild, moderate or severe) . This data was correlated to the known native valvular pathology in hopes of elucidating what role antecedent pathology played in the pattern and severity of pannus formation.

Results: Over 300 prosthetic valves were screened and 119 were identified with a clear history of the native valvular disease. We found that post-inflammatory (rheumatic) pathology was the most common, followed by congenital causes, myxomatous degeneration and native valve endocarditis. In 12 cases, severe pannus overgrowth resulting in hemodynamically significant valvular stenosis was identified, 10 of these from patients with history of rheumatic heart disease and 2 from congenital causes. The relative proportion of severe pannus overgrowth from post-inflammatory heart disease patients (>83%) exceeded that expected from its incidence in our population (69%). The proportion of moderate pannus from patients with congenital heart defects was nearly twice that of patients with rheumatic pathology (43 % vs. 24 %). In addition, the proportion of patients with moderate to severe pannus overgrowth was higher in rheumatic and congenital patients compared to those with antecedent myxomatous or infectious etiologies.

Conclusions: In our study, rheumatic heart disease is most frequently associated with severe pannus overgrowth and moderate overgrowth represented nearly half of the valves explanted from patients with congenital heart disease. Together, these results imply that alterations in the structural and functional relationships between the heart and circulation as well as state of the antecedent endocardium may predispose to pannus formation against foreign devices.

210 Virtual Microscopy in Resident Cardiovascular Pathology Training and Competency Assessment: Comparison to Conventional Light Microscopy

AM Cushman-Vokoun, JD Gentry, BW Keenportz, SK Kohl, KR Mathews, CL Nerby, HR Peck, RK Stevens, GA Talmon, SJ Radio. University of Nebraska Medical Center, Omaha, NE.

Background: Virtual microscopy (VM) is becoming a mainstream tool in undergraduate medical education. Although not yet practical for widespread clinical use, the application of VM to test resident competency and enhance their education warrants investigation. Whether VM is comparable to traditional light microscopy (LM) with regard to pathology resident training in cardiovascular pathology is not well established.

Design: Pathology residents were divided into two groups of four, each group containing junior and senior level residents. One group used LM and the other VM to examine seven common cardiovascular slide cases: amyloidosis, myocarditis, endocardial lymphoid infiltrate (Quilty lesion), aortic involvement with Marfan syndrome, arrhythmogenic cardiomyopathy, infective endocarditis and atrial myxoma. After initial testing, each group was allowed to cross over and compare the other method and subsequently, participants were surveyed on different aspects of LM versus VM.

Results: All residents in each group finished the test in 30 minutes or less. The overall average score for the initial VM group was 89.3% correct and 96.4% for the initial LM group. Of the residents using VM, 3 of the 4 incorrectly diagnosed one of the seven cardiovascular cases, each error was committed on a different case. Two of these three errors were repeated by the same resident on later LM review. The fourth resident correctly identified all of the cases. Of the residents using conventional LM, only one resident incorrectly diagnosed one of the seven cases. The remaining three residents correctly diagnosed all seven cases. All four residents using VM felt comfortable making diagnoses, with 2 residents commenting that the VM images were easy to interpret. However, two of the four felt that certain aspects of VM such as image manipulation (orientation and magnification) were cumbersome compared to a glass slide.

Conclusions: The ability to make accurate cardiovascular pathology diagnoses using VM is comparable to that of LM. Diagnostic errors in the initial VM group testing appear to be knowledge rather than technique based. Overall, residents felt reasonably comfortable with the image quality of VM and its ease of use in diagnosis. Expanded use of VM in resident or fellow cardiovascular pathology education and competency assessment appears justified.

211 Arrythmogenic Right Ventricular Dysplasia/Cardiomyopathy: A Clinicopathological Review

D El Demellawy, J Butany. University of Toronto, Toronto, ON, Canada.

Background: Arrythmogenic right ventricular dysplasia/cardiomyopathy (ARVD) is a rare but significant cause of sudden death in young adults. It likely represents a continuum of morphologic features, which are ill understood and often mis-reported, in spite of its unique morphology.

Design: We evaluated 17 new cases (11 recipient transplant hearts, 3 autopsy hearts and 3 endomyocardial biopsies) of ARVD diagnosed at our department from 1997-2005, with emphasis on the clinicopathological features and prognosis.

Results: There were 6 males and 11 females with a mean age of 42 years (±3). The most common complaint was palpitation, and the most frequent ECG findings were non-specific T wave changes and supraventricular tachycardia. No patients had a family history of heart disease. All hearts exhibited cardiomegaly (mean weight 453 grams (±13)), and 14 showed dilatation (9 biventricular and 5 right ventricular). Aneurysmal bulges were present in 14 hearts (13 right ventricular and 1 left ventricular). Multiple foci of near total myocardial replacement by fibroadipose tissue were seen in the right ventricle (RV) in all cases. Similar foci of fibroadipose tissue infiltration in the left ventricle (LV) were noted in 5 cases, predominantly in the subepicardium. The residual RV myocardial fibers were hypertrophied in 8 cases, and were associated with ischemic changes in 3. Nine cases had significant LV hypertrophy with concomitant ischemic changes in 2. Fibrosis occurred in all cases with septal involvement in 3. In the right atrium, fibrosis occurred in 5 cases, myofibril atrophy in one case and patchy lymphohistiocytic infiltrate in one case. Nine cases had focal LV and RV lymphohistiocytic infiltrates with myocarditis in 4 (3 borderline and 1 active). Apoptosis with apoptotic bodies was seen in 2 cases. There was no evidence of viral inclusions in any case. No significant changes were noted in the valves and in the intramural arteries. None of the patients had any significant complications after heart transplantation.

Conclusions: ARVD presents in adults and shows a female predominance. Though the RV is more severely affected, the disease does show biventricular lesions. Right atrial involvement is frequent and may be in keeping with the insight of the disease as an intrinsic defect within the myocytes. The absence of fatty infiltration and inflammatory infiltrate in the septum may argue against myocarditis as the sole etiological agent. To our knowledge this is the largest North American study and the first to report on atrial changes.

212 Increased Acute Cellular Rejection after Dexamethasone Substitution for Methylprednisone in Heart Transplant Recipients

AN Husain, SE Fedson, AB Cochrane, AY Kim, AS Anderson. University of Chicago, Chicago, IL.

Background: Routine heart biopsies are performed for rejection surveillance after heart transplantation. In the first half of 2003, an increase in the incidence and severity of acute cellular rejection was observed. Immunosuppression at the time of heart transplantation routinely includes the use of IV methylprednisolone. Due to a shortage of methylprednisolone in 2003, IV dexamethasone was substituted for methylprednisolone at standard equivalent doses. This retrospective study was undertaken to compare the equivalency of methylprednisolone and dexamethasone in this clinical setting.

Design: Forty-two consecutive patients who received heart transplants between Jan 2002 and Sept 2003 were studied retrospectively. All patients received immunosuppression consisting of a calcineurin inhibitor, mycophenolate mofetil and a glucocorticoid preparation. Eighteen patients received dexamethasone and 24 patients received methylprednisolone. Four patients were excluded since they died within six weeks. Twelve patients transplanted after Sept 2003 were additionally studied for comparison. All biopsies were graded blinded to the treatment protocol, using the International Society for Heart and Lung Transplantation (ISHLT) classification. All mild (1B) and greater scores were considered positive for rejection.

Results: More patients who received dexamethasone at the time of transplant had cellular rejection (12/17 [70%] vs. 14/33 [42%]; p = 0.05). Analysis showed no difference in the number of patients with grade 1B rejection between the dexamethasone and methylprednisolone groups. Ten of 17 patients (59%) who received dexamethasone had focal moderate or greater rejection compared with 11 of 33 (33%) in the methylprednisolone group. Six of 17 (35%) patients in the dexamethasone group developed multifocal moderate rejection while 5 of 33 (15%) did so in the methylprednisolone group. There was no severe rejection.

Conclusions: Peri-operative high-dose dexamthasone use in heart transplant recipients was associated with significantly higher rates of acute cellular rejection. The equivalencies of dexamethasone and methylprednisolone differ from accepted standards when used in pulse doses. Peri-operative use of glucocorticoids may rely on mechanisms that are distinct from those considered in the standard equivalency measures. Pulse dose glucocorticoids are not interchangeable at standard equivalencies.

213 Histological and Immunohistochemical Evaluation of Amyloid in Endomyocardial Biopsies

MT Idrees, P Gorevic, L Miller, JT Fallon. Mount Sinai School of Medicine, New York, NY.

Background: Endomyocardial biopsy is useful in distinquishing restrictive cardiomyopathy from constrictive pericardial disease. Cardiac amyloidosis is a common cause of restrictive cardiomyopathy. However, deposition of several different proteins may result in cardiac amyloidosis and restrictive cardiac disease. Characterisation of the specific amyloid protein in endomyocardial biopsies may indicate a specific underlying condition and may affect the further workup or management of the patient. We compared the routine histological and immunohistochemical characteristics of endomyocardial biopsies showing amyloid deposition to determine if the type of amyloid could be accurately determined.

Design: Thirty endomyocardial biopsies with cardiac amyloid from 1999-2005 were evaluated. All biopsies were routinely processed. In addition to H&E and trichrome stains, 10 micron thick sections were stained with Congo red. Additional 5 micron sections were stained by routine immunohistochemistry for IgG, kappa, lambda, AA protein, P component and prealbumin (transthyretin/TTR) to characterize. All biopsies were evaluated by two pathologists.

Results: All cases showed positive Congo red staining. Two major patterns of interstitial amyloid deposition were seen: perimyocytic and nodular. Twenty-fwo of 30 were perimyocytic, 6 of 30 were nodular and two of the 30 were mixed. Eleven of 22 cases with a perimyocytic patttern also had vascular deposition of amyloid whereas none of the 6 nodular cases had vascular deposition. By immunohistochemistry of 28 cases, 9 were lambda, 7 were kappa, 9 TTR, none had AA protein, and 3 had indeterminate staining. All were positive for P component. Eight of 9 lambda cases were perimyocytic and 1 mixed; 5 of 7 kappa cases were perimyocytic and 2 nodular; and, 4 of 9 TTR cases were perimyocytic, 4 were nodular and 1 mixed. Ten of 11 cases with vascular amyloid were kappa or lambda, and 1 of 11 was TTR.

IMMUNOHISTOCHEMISTRY VS HISTOLOGICAL PATTERN

HISTOLOGICAL PATTERN	LAMBDA	KAPPA	TTR
PERIMYOCYTIC	8/9 (89%)	5/7 (72%)	4/9 (44%)
NODULAR	0/9 (0%)	2/7 (28%)	4/9 (44%)
MIXED	1/9 (11%)	0/7 (0%)	1/9 (12%)

Conclusions: The results show that most endomyocardial biopsies with perimyocytic and blood vessel amyloid deposition are due to either kappa or lambda deposition. TTR amyloid showed variable patterns of deposition but a nodular pattern without blood vessel deposition suggests TTR amyloid. Immunohistochemical studies are warranted in biopsies with amyloid to definitively characterize the type of amyloid present.

214 Cardiac Inflammatory Myofibroblastic Tumor: A "Benign" Neoplasm That May Result in Syncope, Myocardial Infarction, and Sudden Death

E Kling, AP Burke, R Virmani. University of Maryland Medical Center, Baltimore, MD; International Registry of Pathology, Gaithersburg, MD.

Background: Inflammatory myofibroblastic tumor (IMT) of the heart is extremely rare. We report a series of cardiac IMTs, emphasizing the gross, histologic, and clinical features.

Design: We retrospectively examined endocardial-based spindle cell tumors seen in the files of the Armed Forces Institute of Pathology from 1993-2004. Eight were myofibroblastic proliferations without features of sarcoma, myxoma or papillary fibroelastoma. Immunohistochemisty for smooth muscle actin (in all 8 cases) and ALK-1, pancytokeratin, desmin, and S-100 protein (in four cases) was performed.

Results: There were 5 females and 3 males, with a mean age of 19 years (range 2-72). Tumors were located in the right ventricle (3), mitral valve (2), aortic valve (1), and left ventricle (2). Clinical manifestations were syncope, transient ischemic attacks, and/or seizures (2); cardiopulmonary signs and symptoms (incidental heart murmur (1), dyspnea on exertion (2), myocardial infarction (1); chronic fevers and myalgias (1); and sudden death after unexplained syncopal episodes (1). Cardiopulmonary and neurologic symptoms resulted from prolapse into coronary ostia or embolization of fibrin surface. Imaging studies, when performed, were interpreted as myxoma (3), papillary fibroelastoma (1); in the case with sudden death, echocardiogram had been interpreted as normal. Grossly, the tumors were polypoid or filiform, without papillations, and the cut surfaces were either fibrous or myxoid. Microscopically, tumor cells were spindled to stellate myofibroblasts with abundant cytoplasm in a proteoglycan-rich stroma without significant pleomorphism or cellularity. Mitotic figures were not abundant, necrosis was absent in all cases, and surface fibrin was present in all but one case. Myxoma cells forming vasoformative rings, syncytia, and cords were absent and the lesions were easily distinguished from papillary fibroelastoma by the presence of vessels, inflammation and stellate myofibroblasts within the lesion. Tumor cells were actin positive, and ALK-1, S-100, pancytokeratin, and desmin negative.

Conclusions: Cardiac IMT, although biologically benign, is a distinctive endocardial-based tumor that may result myocardial infarct, syncope, and sudden death. Histologic features are distinctive from the more common myxoma and papillary fibroelastoma. The relationship between cardiac IMT and IMT of soft tissue remains to be determined.

215 Plaque Morphology and Healing of Coronary Thrombi in Sudden Death

E Ladich, K Skorija, S Rittersma, A Burke, R Kutys, Y Liang, M Joner, F Kolodgie, R Virmani. CVPath, International Registry of Pathology, Gaithersburg, MD; Academic Medical Center, Amsterdam, Netherlands.

Background: Analysis of coronary thrombi from patients with acute ST-elevation suggest that thrombus formation is initiated days or weeks before the onset of symptoms (Rittersma SZH et.at., Circulation 2005;111:1160-1165). Although coronary thrombosis is mainly attributed to plaque rupture or erosion, the role of underlying plaque morphology on thrombus propagation and healing has not been characterized.

Design: From a continuing registry of sudden coronary deaths, 98 cases with coronary thrombosis from plaque rupture or erosion were selected for study. Thrombus age was assessed by histology as <1 day (layered platelets and fibrin with trapped granulocytes), 1 to 3 days (as above with nuclear fragmentation), 4 to 7 days (invading smooth muscle cells), and >7 days (organized thrombus). Morphometric parameters including diameter stenosis, plaque burden, and percent necrotic core area were measured at rupture or erosion sites and lesions proximal and distal to the ends of the thrombus.

Results: Most patients were males (82%) with a mean age of 48±10 years. Thrombosis with plaque rupture was found in 62 (63%) of cases with remaining 36 (37%) erosions. The majority of lesions (52%) were localized to the LAD. The number of cases with thrombus age <1 day was 46%, 1 to 3 days (21%), 4 to 7 days (23%), and >7 days (10%).

The mean thrombus length was 9.2±4.8 mm. Overall plaque burden and percent diameter stenosis in lesions with thrombi was independent of thrombus age. In contrast, mean necrotic core area was significantly larger in plaques with thrombi ≤ 3 days as compared with older thrombi. Further, necrotic core area was greatest at rupture sites compared with the proximal and distal lesions while core size in erosions was minimal (<3.5%).
Conclusions: The results confirm earlier findings of older thrombi in acute coronary events as 54% of sudden coronary deaths showed thrombi > 3 days old. Necrotic core size was greatest at rupture sites versus adjacent proximal and distal lesions. Although thrombus age was not related to plaque burden or diameter stenosis, necrotic core size decreases as the thrombus heals.

216 Pericardial Valves – Modes of Failure

V Nair, JW Butany. University Health Network, Toronto, ON, Canada; University of Toronto, Toronto, ON, Canada.
Background: The Carpentier- Edwards Pericardial valve (CEP) is a second generation pericardial valve, has excellent hemodynamics and flow characteristics. Unlike the first generation pericardial valves which failed prematurely because of design problems, the CEP has a long implant life with few reports of its modes of failure. We present an analysis of 23 explanted failed CEP seen by us.
Design: A total of 1042 CEP (aortic and mitral) have been implanted at our institution from 1991 to 2005, 23 of these (from 20 patients) have been surgically explanted at surgery. We report the morphological features and clinical pathological correlations in the 23 explanted CEP seen by us over a 15 year period. All explanted CE P were fixed in formaldehyde, photographed and examined in detail (Gross and Histology).
Results: Mean patient age at implantation was 65.7±14.7 years and 69.9±11.4 years at explantation , (mean duration of 4.2± 5.0 years). There were 15 males and 5 females. Primary tissue deterioration, characterized by degeneration was seen in 26.1% (n=5) of the valves. Cusp tears were seen in 30.4% (n=7) of the explanted valves and the average age of implant duration in these CEP was 10 to 15 years. Pannus was seen in 69.6% (n=16). If the early (<1 year) explants , (7 for infection and perivalvular leak) are excluded, then , 100%(n=16)of the CEP showed pannus, though 12.6 % (n=2) of the valves showed grade 3 and 4 pannus, (both from mitral site, patients had mitral valve conserving procedure). Calcification was seen in 26.1 % (n=6) of explanted valves. Three of the valves showed plate like or diffuse nodular calcification and had been in place for 15 years. Infective endocarditis was seen in 13.0%(n=3), (within 4 months postimplantation).
Conclusions: The CE Pericardial with its significant design changes, (compared to first generation pericardial valves, has a larger effective orifice area, lower residual gradient and a higher closing volume). The incidence of structural valve degeneration was 26.08% at 10 years compared to 90% at 8 years for TSPV, 71% for Ionescu-Shiley bioprosthesis implanted for 5 years and 56% for Hancock II valves at 5.1 years. Cusp tears, were seen in 35% of the cases at 10 years post implant, and calcification in 26.1% (n=6). Pannus was more severe in cases undergoing the mitral conserving procedure. The CEP has a different long term mode of failure, with cusp calcification and valve stenosis the likely cause, rather than valve incompetence, as seen in most porcine bioprostheses.

217 The Effects of Statins on Human Coronary Atherosclerosis

SD Reilly, SH Litovsky, JB Caulfield. University Hospital, Birmingham, AL.
Background: The beneficial effects of statin therapy on human coronary atherosclerosis have been inferred from animal and tissue culture studies and from radiographic studies in humans. The objective of this study is to demonstrate directly the benefits of statin therapy on human coronary atherosclerosis.
Design: We evaluated histologically the coronary arteries in explanted hearts of 33 study patients and 11 controls of patients with coronary artery disease who underwent cardiac transplantation for end stage ischemic heart disease. Myocardial infarction served as indirect proof of the presence of at least one vulnerable plaque at the time of infarction in patients treated with statin therapy. All of the study patients received statin therapy prior to transplant and all of the control patients were selected from the pre statin therapy era.
Results: Two hundred and one sections of coronary arteries were available for review on the thirty-three patients selected (range one to eleven per patient). All patients had plaques and 162 plaques were evaluated. Six plaques (3.7%) in five patients exhibited only intracellular lipid deposition, which was in macrophages. Eighteen plaques (11%) in eight patients exhibited inflammation without intracellular or extracellular lipid and seven (4.3%) plaques in five patients exhibited both lipid deposition in macrophages and inflammation. All of the plaques with lipid deposition showed only small amounts of lipid and all had well developed dense fibrous caps. One hundred thirty one plaques (81%) in sixteen patients (48%) exhibited only dense fibrous plaques, although the presence of healed myocardial infarctions implies the presence of one or more vulnerable plaques at an earlier time. None of the 162 plaques evaluated met the criteria for vulnerable plaques. Seventy sections of coronary arteries were available for review on the eleven control patients selected (range 1 to 28 per patient). All vessels had plaques and seventy plaques were evaluated. Forty-seven plaques met the criteria for vulnerable plaques; all control patients had vulnerable plaques (range 1 to 22 per patient).
Conclusions: The findings in this study support the conclusion that vulnerable plaques will regress during statin therapy transforming lipid laden, inflamed plaques with thin fibrous caps into dense fibrous plaques with reduced to no inflammation which correlates with the decrease in acute coronary events documented in patients who receive statin therapy.

218 Clinicopathologic Correlation of Postmortem BNP Measurement

PA Rodriguez Urrego, D Chua Ang, J Friedman, E Cadoff, BS Fyfe-Kirschner. Robert Wood Johnson Medical School- University of Medicine and Dentistry of New Jersey, New Brunswick, NJ; Cancer Institue of New Jersey, New Brusnwick, NJ.
Background: Serum BNP (sBNP) elevation is seen in congestive heart failure and septic shock. There is no data regarding its applicability in the post-mortem (PM) setting. The purpose of this current study is to demonstrate that sBNP can be measured in PM serum, and to correlate sBNP with clinicopathologic categories of cause of death as well as pattern of BNP immunostaining in autopsy hearts.
Design: BNP was measured in post-mortem serum from 19 patients utilizing a two-site immunoenzymatic assay (Triage BNP test/Biosite Inc). Myocardial tissue from autopsy was immunostained for BNP (Rabbit anti-BNP 32 human serum, Phoenix Pharmaceuticals, Inc). The pattern (perinuclear/diffuse), intensity (0 to 3+) and distribution (transmural, patchy and subendocardial) of staining were then correlated with clinicopathological data.
Results: Nine men and ten women with full PM examination, ranging in age from 38-92 years were grouped into four clinicopathologic categories according to cause of death: cardiovascular disease (CVD) without infection, infection with underlying CVD, infection without underlying CVD and non-CVD/non-infectious cause of death. The results are tabulated . Elevated BNP (>100 pg/ml) was limited to patients with CVD and infection with underlying CVD. Intense strong staining of LV was also limited to these two categories. None of the patients without CVD had a positive sBNP or strong positive BNP staining.
Conclusions: sBNP measurement is useful and technically feasible in the PM setting. Elevations correlate with death due to CVD or infection with underlying CVD. Elevated levels also correlate with strong immunostaining of LV. sBNP is a useful adjunctive tool in the PM setting. As with all studies it must be correlated with all available clinical and pathologic data.

BNP CLINICOPATHOLOGIC CORRELATION

CAUSE OF DEATH	CASES	POSITIVE sBNP	LV BNP IHC (2/3+)	LV BNP IHC (trace/1+)
CVD without infection	6	100% (N=6)	50% 9 (N=3)	50% (N=3)
Infection with underlying CVD	9	88.8% (N=8)	66.6% (N=6)	33.3% (N=3)
Infection without underlying CVD	1	0% (N=0)	0% (N=0)	100% (N=1)
Other causes (non CVD-non infectious)	3	0% (N=0)	0% (N=0)	33.3% (N=1)

CVD: Cardiovacular disease; sBNP: serum Brain Natriuretic Peptide; LV BNP IHC: Left Ventricle BNP Immunohistochemistry

219 Presence of a CD21+ Follicular Dendritic Cell (FDC) Network Distinguishes Invasive Quilty Lesions from Acute Cellular Rejection

HA Sattar, AN Husain, T Krausz. University of Chicago Hospitals, Chicago, IL.
Background: First described by Billingham, Quilty lesions arise in the majority of cardiac transplant patients. Neither the etiology nor the importance of these endomyocardial infiltrates has been fully elucidated. What is clear, however, is that invasive Quilty lesions are diagnostic challenges that mimic acute cellular rejection resulting in inter-observer variability and over-diagnosis of rejection. To date, there exists no definite means of distinguishing these lesions from rejection. Quilty lesions are characterized by capillary-sized blood vessels and a central aggregate of B-cells with a rim of T-cells, an organization similar to the primary follicle of a lymph node. We hypothesized that the organization of invasive Quilty lesions is dependent upon an underlying FDC network, and that the presence of such a network is useful in distinguishing it from cellular rejection.
Design: Consecutive cases of acute cellular rejection (n=25) and invasive Quilty (n=23) for which adequate tissue was available were collected from the pathology archives. The specimens consisted of endomyocardial biopsies taken from transplant recipients over a one-year period (2004-2005). Hematoxylin and eosin staining was used to establish the diagnoses. A single unstained section was immunostained for CD21 to investigate the presence of a FDC network.
Results: A compact CD21+ FDC network was present in 15 of the 17 invasive Quilty lesions that were 0.3mm or larger in greatest dimension ($p<0.00001$), and was completely absent in all 25 lesions of acute cellular rejection (G1A/1B, n=7; G2, n=13; G3A/3B, n=4; G4, n=1). Of the 8 invasive Quilty lesions that lacked an FDC network, 6 measured less than 0.3mm (n=6) and the remaining 2 were between 0.3 and 0.4mm. When present, the follicular dendritic cells were in the center of the lesion and the number of positive cells was proportional to the size of the lesion, likely explaining the lack of staining for the FDC-network in some of the smaller lesions.
Conclusions: The presence of a CD21+ FDC network reliably distinguishes invasive Quilty lesions from acute cellular rejection, especially in those lesions (>0.3mm) that are most likely to be over-diagnosed as moderate or severe acute cellular rejection (sensitivity 88%, specificity 100%, positive predictive value 100%). Use of CD21 immunoreactivity to highlight this network would be of benefit in reducing the rate of over-diagnosis known to be associated with invasive Quilty lesions, alleviating unnecessary immunosuppresion and its associated risks.

220 Complement Regulatory Proteins Play a Role in the Clinical Presentation of Antibody-Mediated Rejection

CD Tan, GV Gonzalez-Stawinski, NG Smedira, RC Starling, ER Rodriguez. The Cleveland Clinic Foundation, Cleveland, OH.
Background: Antibody-mediated rejection (AMR) in heart transplants is a clinical entity with a which occurs in 3% of non-sensitized patients and approximately 20% of sensitized patients. The hallmark of AMR is the activation and deposition of complement in the myocardial capillaries which, in turn, is followed by dysfunction of the allograft of frank heart failure. In some patients the activation of complement is not accompanied

by dysfunction of the allograft. **Hypothesis**: Activation of complement in cardiac allograft recipients without allograft dysfunction may indicate that a protective mechanism exists.
Design: Endomyocardial biopsies from 8 patients with complement deposition were compared. Four patients survived these episodes of AMR and 4 did not. Immunofluorescence staining of the endomyocardial biopsies was performed with the following markers: CD35 (Complement receptor 1, CR1), CD46 (Membrane Cofactor Protein, MCP), CD55 (Decay Accelerating Factor, DAF) and CD59 (Protectin). These markers are complement regulatory proteins which play a role in controlling and silencing complement activation and tissue injury or in removing complement complexes.
Results: Patients with good response to therapy and resolution of the AMR episode showed intense tissue expression of these complement regulatory proteins in the endothelium of the allograft. Patiens with poor outcome had low or absent tissue expression of complement regulatory proteins.
Conclusions: Local expression of complement regulatory proteins on the endothelial cell surface plays a role in controlling the deleterious effects of complement activation during episodes of AMR . Identification of these regulatory proteins in tissue and understanding of the mechanisms that control their expression will be a useful tool to predict outcome

221 Allograft Inflammatory Factor-1 (AIF-1) Immunohistochemistry Stain in Biopsies of Human Heart Transplants

X Zhou, Z He, J Henegar, S Bigler, B Allen. University of Mississippi Medical Center, Jackson, MS.

Background: Allograft inflammatory factor-1 (AIF-1) is a 143-amino acid, Ca^{++}-binding protein originally identified in rat models of cardiac allograft rejection, and subsequently identified in a variety of chronic inflammatory conditions in humans. Immunohistochemistry was used to investigate the distribution of AIF-1 expression in endomyocardial biopsies of transplanted and native human hearts.
Design: Endomyocardial biopsy samples during the period of 2003-2005 from 36 transplanted and 17 native hearts were studied. The median age of the transplant patients was 42 (range, 14-64 years), the non-transplanted patient median age was 29 (range, 7-68 years), and the median time post-transplantation was 12 months (range, 1 week-11 years). Rejection was graded according to ISHLT criteria in the transplanted hearts, with 5 grade 0, 8 grade 1, 7 grade 2, and 16 grade 3 cases. The 17 native hearts showed a variety of findings including idiopathic dilated cardiomyopathy, hypertrophic cardomyopathy, amyloidosis, endocarditis, or no diagnostic findings. Immunohistochemistry was performed using paraffin-embedded, formalin fixed tissue sections with a primary mouse monoclonal antibody, purchased from ABcam (clone #1022-5) using standard avidin biotin conjugate techniques with peroxidase and DAB substrate (Vectastain ABC Kit from Vector Laboratories). The primary antibody was diluted to a concentration of 2 μg/ml. Immunostaining was graded in mononuclear cells and cardiac myocytes: 0 (no staining), 1 (focal, few cells staining), 2 (patchy staining less than 50% of cells), and 3 (extensive staining, more than 50% of cells).
Results: Infiltrating mononuclear cells in transplanted hearts expressed AIF-1. In hearts with worse rejection, the infiltrates were more extensive, and there was greater reactivity of the cells ($p<0.00001$, ANOVA with $F=19$). Perinuclear staining of cardiac myocytes was also observed and correlated with the degree of rejection ($p<0.013$, ANOVA with $F=3.534$). There was no significant difference between the staining of lymphocytes in Quilty lesions and infiltrating parenchymal mononuclear cells associated with myocyte damage. The non-transplanted hearts had very few parenchymal mononuclear cells, and showed little to no expression of AIF-1.
Conclusions: AIF-1 expression is common in cellular rejection of transplanted hearts, involving both infiltrating mononuclear cells and cardiac myocytes.

Cytopathology

222 The Role of Peroxisome Proliferator Activated Receptor Gamma (PPARγ) Staining in the Cytopathological Diagnostic Value in Follicular Neoplasm's of the Thyroid Gland

M Abdelbaqi, Y Dancer, E Turbat-Herrera. Louisiana State University, Shreveport, LA.

Background: The PAX8 gene belongs to a family of genes that plays a critical role in the formation of tissues and organs, such as kidney and thyroid gland during embryonic development. It is also important for maintaining the normal function of certain cells after birth. PAX8 proteins act as transcription factors by binding to specific area of DNA. The peroxisome proliferator activated receptors (PPARs) are ligand-dependent transcription factors that belong to a nuclear hormone superfamily. It is created by somatic tumor genetic translocation between chromosome arm 2q and 3p. This translocation t (2; 3)(q13; p25), leading to the formation of a chimeric PAX8-PPAR receptor oncogene. This leads to fusion of the the entire coding region of the nuclear transcription factor gene PPAR in-frame with the first six to nine exons of the PAX8 gene, which encodes for a thyroid specific-specific paired box transcription factor. Several reports have indicated that PAX8-PPARγ is detected in follicular thyroid carcinomas (FTC), but not in follicular thyroid adenomas (FTA), papillary thyroid carcinomas (PTC), or multinodular hyperplasias. However, to our knowledge there have been no reports that have studied this problem using cytology. In this study we propose to compare the IHC for PPARγ in surgical and FNA specimens to improve the diagnosis and classification.
Design: A total of 34 fine needle aspirates cases of follicular neoplasm, including 10 cases of FTA, 12 cases of classical FTC/follicular variant of PTC, and 12 cases of nodular hyperplasias. Including the corresponding surgically resected specimens and cell blocks. Immunostaining with PPARγ (mouse monoclonal antibody, Santa Cruz, Ca) was performed. The staining pattern was assesed by two independent pathologists. Cases were graded as positive if nuclear membranes stain is detected.
Results: Our results have showed a positive nuclear staining pattern in cases of follicular thyroid carcinoma,while the cases of follicular thyroid adenoma and nodular hyperplasia have tested negative.
Conclusions: PPARγ nuclear immunostaining can be useful as an adjunct to the FNA of the thyroid. PPARγ immunostaining can help differentiate between Follicular thyroid carcinoma and Follicular thyroid adenoma.

223 Correlation of Cytologic Examination with ELISA Assays for Hyaluronan and Soluble CD44v6 Levels in Evaluation of Effusions

A Afify, L Lynne, L Howell. University of California Davis Medical Center, Sacramento, CA.

Background: Hyaluronan (HA) and its major cell surface receptors, CD44 play an important role in tumor growth, neovascularization, and invasion. CD44 is an integral transmembrane protein and exists in standard form as well as variants isoforms (CD44v1-v10). Functional fragments of the CD44 can be released from the cell membrane by proteolytic cleavage of extracellular domain producing soluble CD44. Although studies have proposed the use of serum HA and soluble CD44 specifically CD44v6 levels as a tumor markers, its diagnostic utility in body fluid samples has not been established. The purpose of this study was to correlate HA and soluble CD44v6 levels in effusions with the cytology diagnosis and to assess their usefulness in differentiating malignant from non-malignant effusions.
Design: In this prospective study we evaluated HA and soluble CD44v6 contents in 20 effusions from cytologically positive samples (18 metastatic adenocarcinomas and 2 lymphomas) and 10 effusions from cytologically negative samples. Corresponding cytopathology slides were reviewed to confirm the diagnosis. The level of HA and soluble CD44v6 were measured using a sandwich enzyme-linked immunoadsorbent assay. For HA we used Hyaluronic Acid Quantitative Test kit (Corgenix, Denver) and for soluble CD44v6 we used Human sCD44v6 Instant ELISA (Bender MedSystems, Vinna, Austria). HA concentrations (ng/L) and soluble CD44v6 concentrations (ng/mL) were calculated and correlated with clinical data as well as cytodiagnosis.
Results: The mean concentration of HA (22.42±5.04 ng/L) and soluble CD44v6 (99 ±132 ng/mL) in the cytologically positive samples was significantly higher than those in the cytologically negative samples for HA (5.5 ±5.04ng/L, $P<0.01$) and soluble CD44V6 (17 ±10 ng/Ml, $p= 0.013$). Using benign effusions as control and the upper limits of its mean levels for HA (10.5 ng/L) as positive boundary value, HA level exceeded the boundary line in 17 out of 20 malignant effusions cases and 2 out of 10 benign effusions cases. Meanwhile CD 44v6 exceeded the boundary line (27 ng/mL) in 18 out of 20 malignant effusions cases and 3 out of 10 benign effusions cases. The calculated sensitivity and specificity of this assay to the diagnosis of malignant effusions were 85% and 80% for HA and 90% and 70% for CD44v6 respectively.
Conclusions: We conclude that the HA and soluble CD44v6 levels in body fluids correlate with the cytology diagnosis and could be used as an ancillary study in cytology to differentiate non-malignant from malignant effusions.

224 Diagnostic Utility of CD44 Standard, CD44v6, and CD44v3-10 Expression in Adenocarcinomas Presenting in Serous Fluids

A Afify, L Pang, L Howell. University of California Davis Medical Center, Sacramento, CA.

Background: CD44 is an 85-90 kDa integral transmembrane protein encoded by a single 20 exon gene. In the standard form (CD44s) ten of the 20 exons are transcribed. Multiple variant isoforms exist (CD44v1-v10) which arise from alternate mRNA splicing of the remaining 10 exons. In contrast to the standard form of CD44, which is almost ubiquitously expressed, splice variants are highly restricted in their expression in normal or malignant tissues. The purpose of this study was to evaluate the extent to which adenocarcinomas express CD44s, CD44v6 and CD44v3-10 in fluids and to assess their diagnostic utility in distinguishing reactive mesothelial cells from adenocarcinomas in body cavity fluid.
Design: Archival paraffin-embedded cell blocks of serous fluids from 23 cases of benign effusions containing reactive mesothelial cells and 45 cases of malignant effusions with metastatic adenocarcinoma (18 ovarian, 11 pulmonary, 9 gastrointestinal, and 7 breast) were retrieved from the cytopathology files. The cytopathology of all cases was reviewed to confirm the diagnosis. Immunohistochemistry was performed on all cases using antibodies for CD44s, CD44v6 and CD44v3-10 (Bender MedSystems, CA). Positive staining was defined as distinct linear membrane staining. Strong staining in at least 10% of the tumor cells was required in order to consider the case positive for the particular marker.
Results: In benign effusions mesothelial cells expressed CD44s in 22 cases (96%), CD44v6 in 2 cases (9%) and CD44v3-10 in 2 cases (9%). In contrast neoplastic cells in malignant effusions expressed CD44s in 14 cases(31%), CD44v6 in 21 cases (47%), and CD44v3-10 in 34 cases (76%). Meanwhile malignant cells demonstrated either or concurrent reactivity for CD44v6 and CD44v3-10 in 38 cases (84%).

The IHC results of adenocarcinomas

	CD44s	CD44v6	CD44v3-10
Ovarian Aca (n=18)	2(11%)	4(22%)	14(78%)
Lung Aca (n=11)	7(64%)	9(82%)	7(64%)
GI Aca (n=9)	2(22%)	4(44%)	8(89%)
Breast Aca (n=7)	3(43%)	4(57%)	5(71%)
Total(n=45)	**14 (31%)**	**21(47%)**	**34 (76%)**

ACa:adenocarcinomas; GI:gastrointestinal

Conclusions: CD44s, CD44v6 CD44v3-10 are useful markers that can be applied to cytologic specimens. CD44s immunostaining can be used as a reliable marker to identify reactive mesothelial cells while the combination of CD44v6 and CD44v3-10 immunostaining can detect majority of adenocarcinomas in malignant effusions.